

Fast Lossless Compression with Integer-Only Discrete Flows

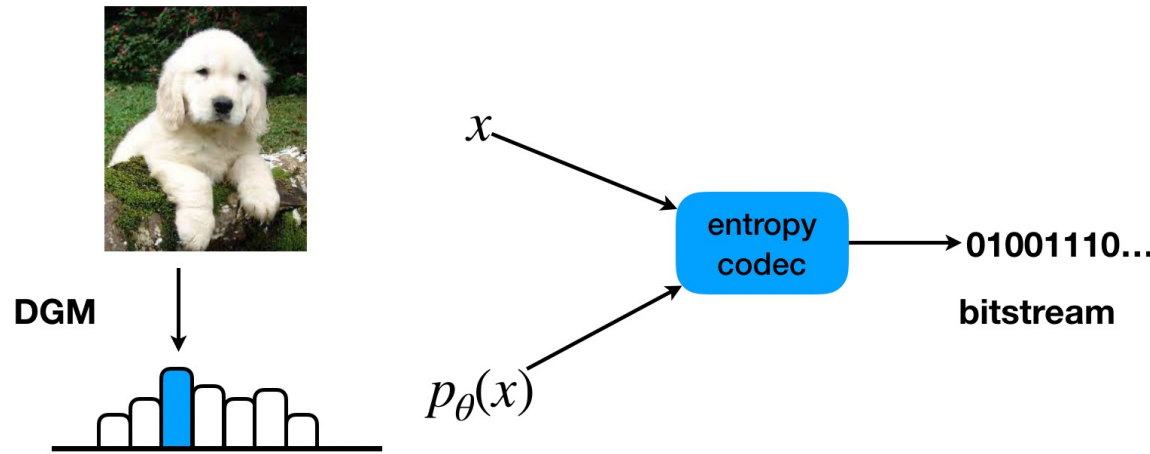
Siyu Wang¹, Jianfei Chen¹, Chongxuan Li², Jun Zhu¹, Bo Zhang¹

¹Tsinghua University; ²Renmin University of China

Background

DGM For lossless compression

Neural Compressor: Probabilistic Model + Entropy Coding



High compression rate

Low encoding/decoding speed

Background

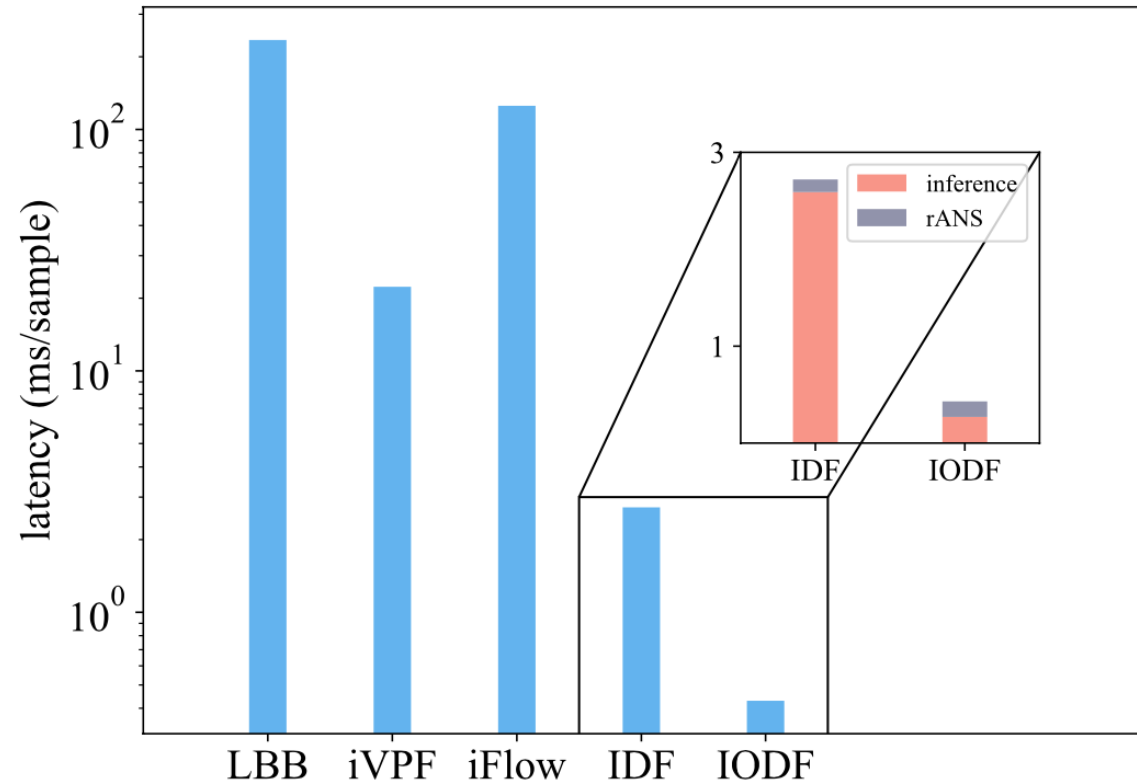
Integer discrete flows (IDF, *Hoogeboom et al.*)

Model data x and latent representation z both in discrete integer space:

$$\mathcal{X} = \mathcal{Z} = \mathbb{Z}^d$$

Design a bijective function $f_\theta(\cdot)$ between x and z . With change-of-variable formula,

$$P_X(x) = P_Z(f_\theta(x))$$



Method

Quantization

Hybrid format representation

Tensors are represented with a hybrid numerical format, which is done by a *quantizer* Q .

For a real-valued tensor \mathbf{r} , the quantizer outputs

$$\tilde{\mathbf{r}} = Q(\mathbf{r}) = s_{\mathbf{r}} \hat{\mathbf{r}} \approx \mathbf{r}$$

$\hat{\mathbf{r}}$: 8-bit integers in $\{-128, \dots, +127\}$ or $\{0, \dots, +255\}$.

$s_{\mathbf{r}}$: scalar, scale parameter.

Method

Quantization

Convolution $\mathbf{y} = \text{Conv}(\mathbf{x}; \mathbf{W}, \mathbf{b})$

\mathbf{W} is a $C \times D \times k \times k$ convolution kernel, \mathbf{b} is a C -dimensional bias vector,
 \mathbf{x} is a $D \times h \times w$ input tensor, and \mathbf{y} is a $C \times h' \times w'$ output tensor.

$$y_c = \sum_{c'=1}^D W_{c,c'} \circledast x_{c'} + b_c, \quad c \in \{1, \dots, C\}$$

Method

Quantization

Integer-only Convolution

Use hybrid format to represent $\mathbf{y}, \mathbf{x}, \mathbf{W}$ $\mathbf{y} \approx s_{\mathbf{y}} \hat{\mathbf{y}}, \mathbf{x} \approx s_{\mathbf{x}} \hat{\mathbf{x}}, \mathbf{W} \approx s_{\mathbf{W}} \hat{\mathbf{W}}$.

plug them into

$$y_c = \sum_{c'=1}^D W_{c,c'} \circledast x_{c'} + b_c, \quad c \in \{1, \dots, C\}$$

reorganize terms, we have

$$\hat{y}_c \approx \frac{s_{\mathbf{W}} s_{\mathbf{x}}}{s_{\mathbf{y}}} \sum_{c'=1}^D \hat{W}_{c,c'} \circledast \hat{x}_{c'} + \frac{b_c}{s_{\mathbf{y}}}.$$

Method

Quantization

$$\tilde{\mathbf{r}} = Q(\mathbf{r}) = s\hat{\mathbf{r}} = s \cdot \left[\text{clip} \left(\frac{\mathbf{r}}{s}, -Q_N, Q_P \right) \right]$$

Learned Step-size Quantization (LSQ, Esser *et al.*)

Back-propagation through quantizer is performed with STE (Bengio *et al.*): $\partial [\mathbf{u}] / \partial \mathbf{u} = \mathbf{I}$

$$\frac{\partial \mathcal{L}}{\partial \mathbf{r}} = \frac{\partial \mathcal{L}}{\partial \tilde{\mathbf{r}}} \frac{\partial \tilde{\mathbf{r}}}{\partial \mathbf{r}} = \frac{\partial \mathcal{L}}{\partial \tilde{\mathbf{r}}}, \quad \mathbf{r} = \mathbf{W} \text{ or } \mathbf{x},$$

Gradient of scale parameter s

$$\frac{\partial \tilde{\mathbf{r}}}{\partial s} = \begin{cases} (-\mathbf{r}/s + \lfloor \mathbf{r}/s \rfloor) \odot \mathbb{I}(-Q_N < \mathbf{r}/s < Q_P) \\ -Q_N \cdot \mathbb{I}(\mathbf{r}/s < -Q_N) \\ Q_P \cdot \mathbb{I}(\mathbf{r}/s > Q_P) \end{cases} \quad \frac{\partial \mathcal{L}}{\partial s} = \frac{\partial \mathcal{L}}{\partial \tilde{\mathbf{r}}} \frac{\partial \tilde{\mathbf{r}}}{\partial s}$$

Method

Quantization

Deployment on GPU

After fine-tuning networks with fake quantizers, we deploy the model on GPU with TensorRT library and realize more efficient inference.

Improvement of network architecture

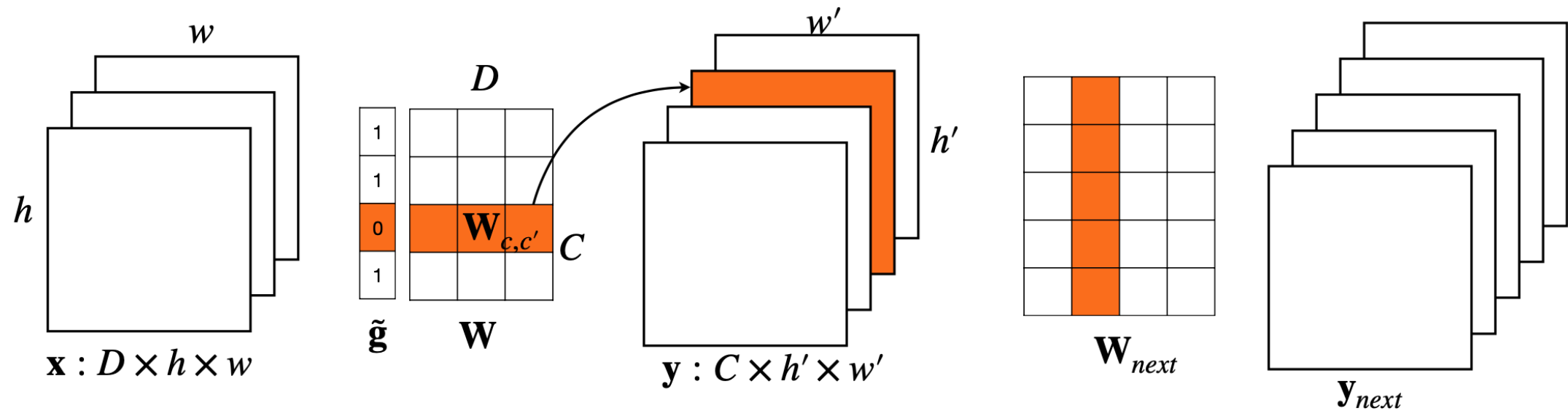
- Dense blocks v.s.residual blocks
- Optimization over residual blocks

Table 1. Latency of floating-point and integer-only inference for convolutions with varying number of input and output channels. Obtained by averaging over 1000 runs (milliseconds).

| IN CHN | OUT CHN | FP32 | INT8 | SPEEDUP |
|--------|---------|-------|--------|---------|
| 128 | 128 | 0.040 | 0.0039 | 10.2× |
| 64 | 256 | 0.035 | 0.0098 | 3.6× |
| 32 | 512 | 0.037 | 0.0131 | 2.8× |

Method

Pruning



Method

Pruning

Training binary-gated convolution

$$\mathcal{L}(\mathbf{X}; \{\mathbf{W}\}, \{\mathbf{g}\}) = \mathcal{L}_{IDF}(\mathbf{X}; \{\mathbf{W}\}, \{\mathbf{g}\}) + \sum \lambda \|\tilde{\mathbf{g}}\|_1,$$

\mathcal{L}_{IDF} tends to remain all entries of $\tilde{\mathbf{g}}$ close to 1 to remain high performance.
 $\|\tilde{\mathbf{g}}\|_1$ pushes the gates to be sparse.

Method

Training workflow

Algorithm 1 Training IODF

Input: r_{target} , remaining target proportion of FLOPs and \mathbf{X} , the training dataset.

#Stage 1:

$\mathbf{W} \leftarrow \text{InitializeParameter}()$

Train $\mathcal{L}_{IDF}(\mathbf{X}; \{\mathbf{W}\}, \{1\})$ to convergence

$F_0 \leftarrow \text{CalculateFLOPs}(\mathbf{W})$

#Stage 2:

$\mathbf{g} \leftarrow \alpha \mathbf{1}$, $\lambda \leftarrow \text{InitializeLambda}()$

Train $\mathcal{L}(\mathbf{X}; \{\mathbf{W}\}, \{\mathbf{g}\})$ until $\text{CalculateFLOPs}(\mathbf{W}, \mathbf{g}) <$

$r_{target} F_0$

#Stage 3:

Fine-tune $\mathcal{L}_{IDF}(\mathbf{X}; \{\mathbf{W}\}, \mathbf{g})$ with fixed \mathbf{g}

#Stage 4:

Fine-tune the model with fake quantization applied to activations

#Stage 5:

Fine-tune the model with fake quantization applied to activations and weights

| | ANALYTIC BPD | CODING BPD | 4 | 8 | 16 | 32 | 64 | 4 | 8 | 16 | 32 | 64 |
|-------------------|-----------------|---------------|-------|-------|-------|------|------|------|------|------|------|------|
| IMAGENET32 | | | | | | | | | | | | |
| IDF-DENSE | 3.890 | 3.900 | 8.38 | 5.08 | 4.08 | * | * | 0.31 | 0.54 | 0.70 | * | * |
| IDF-RES | 3.916 | 3.926 | 4.19 | 3.19 | 3.59 | 2.54 | 2.93 | 0.56 | 0.79 | 0.79 | 1.12 | 1.00 |
| 8BIT IDF-DENSE | 3.911 | 3.921 | 5.38 | 2.90 | 1.74 | 1.20 | 0.99 | 0.46 | 0.86 | 1.21 | 2.18 | 2.67 |
| 8BIT IDF-RES | 3.923 | 3.934 | 2.08 | 1.09 | 0.64 | 0.44 | 0.36 | 0.91 | 1.78 | 2.96 | 4.76 | 5.98 |
| PRUNED IDF-RES | 3.936 | 3.947 | 3.27 | 2.04 | 1.60 | 1.33 | 1.29 | 0.72 | 1.14 | 1.59 | 2.01 | 2.15 |
| IODE | 3.968 | 3.979 | 1.79 | 0.94 | 0.54 | 0.34 | 0.27 | 0.98 | 1.91 | 3.45 | 5.41 | 7.08 |
| SPEEDUP | - | - | 4.7× | 5.4× | 7.6× | * | * | 3.2× | 3.6× | 4.9× | * | * |
| IMAGENET64 | | | | | | | | | | | | |
| IDF-DENSE | 3.635 | 3.638 | 18.65 | 15.45 | 13.93 | * | * | 0.59 | 0.73 | 0.83 | * | * |
| IDF-RES | 3.637 | 3.640 | 12.50 | 11.89 | 9.30 | 8.84 | 8.64 | 0.82 | 0.93 | 1.22 | 1.32 | 1.35 |
| 8BIT IDF-DENSE | 3.663 | 3.666 | 8.98 | 5.57 | 4.35 | 3.67 | 3.34 | 1.02 | 1.66 | 2.32 | 2.83 | 3.11 |
| 8BIT IDF-RES | 3.663 | 3.673 | 3.03 | 2.02 | 1.61 | 1.41 | 1.31 | 1.83 | 3.47 | 4.72 | 5.57 | 6.83 |
| PRUNED IDF-RES | 3.657 | 3.666 | 7.75 | 6.45 | 6.55 | 5.79 | 5.71 | 1.21 | 1.59 | 1.70 | 1.93 | 2.00 |
| IODE | 3.685 | 3.695 | 2.79 | 1.71 | 1.34 | 1.15 | 1.06 | 2.22 | 3.72 | 4.64 | 7.03 | 7.93 |
| SPEEDUP | - | - | 6.9× | 9.0× | 10.4× | * | * | 3.8× | 5.1× | 5.6× | * | * |

Reference

- Duda, J. Asymmetric numeral systems. arXiv preprint arXiv:0902.0271, 2009.
- Duda, J. Asymmetric numeral systems: entropy coding combining speed of huffman coding with compression rate of arithmetic coding. arXiv preprint arXiv:1311.2540, 2013.
- Ho, J., Lohn, E., and Abbeel, P. Compression with flows via local bits-back coding. arXiv preprint arXiv:1905.08500, 2019.
- Ho, J., Jain, A., and Abbeel, P. Denoising diffusion probabilistic models. arXiv preprint arXiv:2006.11239, 2020.
- Hoogeboom, E., Peters, J. W., Berg, R. v. d., and Welling, M. Integer discrete flows and lossless compression. arXiv preprint arXiv:1905.07376, 2019.
- Huffman, D. A. A method for the construction of minimum-redundancy codes. Proceedings of the IRE, 40(9):1098–1101, 1952.
- Kingma, D. P. and Dhariwal, P. Glow: Generative flow with invertible 1x1 convolutions. arXiv preprint arXiv:1807.03039, 2018.
- Kingma, D. P. and Welling, M. Auto-encoding variational bayes. In International Conference on Learning Representations, 2013.
- Kingma, D. P., Salimans, T., Poole, B., and Ho, J. Variational diffusion models. arXiv preprint arXiv:2107.00630, 2, 2021.
- NVIDIA. Tensorrt. <https://developer.nvidia.com/tensorrt>, 2018.
- Shannon, C. E. A mathematical theory of communication. The Bell system technical journal, 27(3):379–423, 1948.
- Zhang, S., Kang, N., Ryder, T., and Li, Z. iflow: Numerically invertible flows for efficient lossless compression via a uniform coder. Advances in Neural Information Processing Systems, 34, 2021b.
- Nalisnick, E., Matsukawa, A., Teh, Y. W., Gorur, D., & Lakshminarayanan, B. (2018). Do deep generative models know what they don't know?. arXiv preprint arXiv:1810.09136.
- Zhang, S., Zhang, C., Kang, N., and Li, Z. ivpf: Numerical invertible volume preserving flow for efficient lossless compression. In Proceedings of the IEEE/CVF Conference on Computer Vision and Pattern Recognition, pp. 620–629, 2021c.
- Jascha Sohl-Dickstein, Eric Weiss, Niru Maheswaranathan, and Surya Ganguli. Deep unsupervised learning using nonequilibrium thermodynamics. In International Conference on Machine Learning, pages 2256–2265, 2015.
- Dinh, Laurent, Jascha Sohl-Dickstein, and Samy Bengio. "Density estimation using real nvp." arXiv preprint arXiv:1605.08803 (2016).
- Yann LeCun, Sumit Chopra, Raia Hadsell, M Ranzato, and F Huang. A tutorial on energy-based learning. Predicting structured data, 1(0), 2006.
- Jiaming Song, Chenlin Meng, and Stefano Ermon. Denoising diffusion implicit models. arXiv preprint arXiv:2010.02502, 2020a.
- Bao F, Li C, Zhu J, et al. Analytic-DPM: an Analytic Estimate of the Optimal Reverse Variance in Diffusion Probabilistic Models[J]. arXiv preprint arXiv:2201.06503, 2022.
- Zhang M, Zhang A, McDonagh S. On the out-of-distribution generalization of probabilistic image modelling[J]. Advances in Neural Information Processing Systems, 2021, 34.

Thanks for listening.